

MYCN SILENCING BY RNAI INDUCES NEUROGENESIS AND SUPPRESSES PROLIFERATION IN MODELS OF NEUROBLASTOMA WITH RESISTANCE TO RETINOIC ACID

Ruhina Maeshima¹, Dale Moulding², Andrew W Stoker³ and Stephen L Hart^{1*}

1. Genetic and Genomic Medicine Department, UCL Great Ormond Street Institute of Child Health, London, UK
2. UCL Great Ormond Street Institute of Child Health, London, UK
3. Developmental Biology & Cancer Department, UCL Great Ormond Street Institute of Child Health, London, UK

*Corresponding author:

Stephen L Hart

s.hart@ucl.ac.uk

Fax: +44 (0) 20 7905 2810

30 Guilford St, London, UK WC1N 1EH

Keywords: siRNA, Neuroblastoma, *MYCN*, retinoic acid treatment

Running title: Gene therapy by RNAi for Neuroblastoma

ABSTRACT

Neuroblastoma (NB) is the most common solid tumour in childhood. Twenty percent of patients display *MYCN* amplification, which indicates a very poor prognosis. *MYCN* is a highly specific target for a neuroblastoma tumour therapy as *MYCN* expression is absent or very low in most normal cells while, as a transcription factor, it regulates many essential cell activities in tumour cells. We aim to develop a therapy for NB based on *MYCN* silencing by short interfering RNA molecules, which can silence target genes by RNA interference, a naturally-occurring method of gene silencing. It has been shown previously that *MYCN* silencing can induce apoptosis and differentiation in *MYCN* amplified neuroblastoma. In this paper, we have demonstrated that siRNA-mediated silencing of *MYCN* in *MYCN*-amplified neuroblastoma cells induced neurogenesis in NB cells whereas retinoic acid (RA) treatment did not. RA can differentiate NB cells and is used for treatment of residual disease after surgery or chemotherapy, but resistance can develop. In addition, *MYCN* siRNA treatment suppressed growth in a *MYCN*-amplified neuroblastoma cell line more than that by RA. Our result suggests that gene therapy using RNAi targeting *MYCN* can be a novel therapy toward *MYCN* amplified neuroblastoma that have complete or partial resistance toward RA.

INTRODUCTION

Neuroblastoma (NB) is one of the most common solid tumours in early childhood accounting for about 7% of paediatric malignancies and approximately 15% of cancer-related deaths in childhood [1, 2]. Neuroblastoma arises from primitive cells of the neural crest [3], which normally differentiate to form the nervous system and adrenal medulla [4]. Amplification of the proto-oncogene *MYCN* is strongly correlated with a poor prognosis in neuroblastoma, and accounts for approximately 20% of cases. Like other cancers, current NB therapy includes surgery, chemotherapy, monoclonal antibody treatment, and radiotherapy [5]. The NB tumours vary remarkably in their response to treatment based upon their stage and biological features [6]. Even *MYCN*-amplified NB may achieve remission after surgery alone if it remains localised [5]. Chemotherapy treatment with 13-*cis*-retinoic acid has become the standard therapy in high-risk NB which induces neuronal differentiation [7] and maintains NB as a minimal residue disease [8]. However, the emergence of 13-*cis*-retinoic acid resistance eventually leads to relapse in most cases [9]. Supplementation of therapy with anti-GD2 antibody therapies combined with granulocyte macrophage colony stimulating factor (GM-CSF) and interleukin-2 (IL-2) has improved the 2-year survival rate by 20% [7, 10, 11], but for patients developing resistance to retinoic acid, the prognosis of *MYCN*-amplified NB remains very poor [11, 12].

N-Myc is a member of the Myc family and a bHLHZip transcription factor, controlling many genes involved in the regulation of essential cellular activities [13, 14]. Myc proteins, including N-Myc, act as both transcriptional activators and repressors [15-17]. N-Myc also binds at, or around, the transcription start site of genes which have already been transcriptionally activated and amplifies transcription of the genes [18]. Overexpressed N-Myc induces proliferation, and suppresses apoptosis and differentiation and so promotes tumorigenesis of NB [13]. N-Myc is a transcription factor, for which it is typically very difficult to develop drugs, hence, N-Myc is a good potential target for genetic therapy by siRNA-mediated silencing.

Studies on N-Myc expression in adult mice suggest levels that are very low or absent in the brains and other organs, although it is expressed in the forebrain, hindbrain and in kidney of new-born mice [19]. This suggests that a *MYCN*-targeted siRNA therapy is unlikely to have any significant off-target effects since it is unlikely to enter the brain

due to the impermeability of the blood brain barrier. There have been several proof-of concept studies into *MYCN* siRNA therapies [20-23] but none has emerged as a clinical product so far, and further studies are required into the mechanism and safety of this approach.

Short interfering RNA (siRNA) is a naturally occurring method of gene silencing first described in 1998 [24]. Over the last twenty years there have been numerous attempts to develop clinical applications of siRNA and the first siRNA-based drug Patisiran (Onpattro), for transthyretin amyloidosis (TTR), was approved for clinical use by the US Food and Drug Administration (FDA) in August 2018 [25]. RNA interference (RNAi) is a promising approach for cancer therapy and has been used for example, in the knockdown of oncogenes such as neuron growth factor (NGF) in pancreatic cancer [26] and stearoyl-CoA desaturase-1 (SCD1) in liver cancer [27]. Several siRNAs for cancer treatment have entered clinical trials, such as Atu-027 targeting protein kinase N3 gene for therapy of advanced solid tumours, and SPC2996 targeting Bcl-2 gene for chronic lymphocytic leukaemia [28]. While there is undoubted potential for siRNA cancer therapies, problems of delivery have proven difficult to overcome but evidence with Patisiran, involving high-efficiency delivery of siRNA to the liver by lipid nanoparticles (LNPs) [25], reinforces the belief that, if the delivery issue can be solved, there is the prospect for a wide range of novel therapies for cancer.

Thus, in other areas of our research we are developing genetic approaches to therapy of NB with novel nanoformulations based on mixtures of targeting peptides and lipids, that can be delivered systemically. For example, we have delivered plasmid DNA (pDNA) expressing interleukin(IL)-2/IL12 cytokine adjuvant immunotherapies to tumours in the syngeneic murine model of NB, leading to tumour eradication [29, 30]. We have also developed lipid/peptide nanoformulations for siRNA packaging and delivery [31-33] and aim to use this in developing novel NB therapies. In this paper, we have investigated on the therapeutic potential of *MYCN* silencing by RNAi in *MYCN* amplified NB cells *in vitro*, focusing on the potential for treatment of disseminated, RA-resistant tumours. We have further investigated the hypothesis that *MYCN* silencing by siRNA could limit proliferation and promote differentiation of NB cells by analysing the expression of proteins involved in differentiation, in cell replication and in the production of neurites, characteristic of differentiated neurons. The results of this study

are a key step towards the development of the therapeutic potential of MYCN siRNA, that will enable us to progress to therapeutic studies *in vivo*.

Materials and Methods

Cell culture

Human *MYCN*-amplified NB cell lines Kelly and SK-N-BE(2) were cultured in RPMI1640+GlutaMAX (Thermo Fisher Scientific, Northumberland, UK) with 10% Foetal Bovine Serum (FBS) (Sigma-Aldrich, Dorset, UK), 25 mM HEPES buffer, and 100 U/mL Penicillin/Streptomycin (P/S) (Thermo Fisher Scientific, Northumberland, UK). Non *MYCN*-amplified cell lines LAN-5 and SK-N-SH cells were cultured in Minimum Essential Medium Eagle (MEM, Sigma-Aldrich, Dorset, UK) with 10% FBS, 2mM L-glutamine (Thermo Fisher Scientific, Northumberland, UK) and 100 U/mL P/S.

siRNA

The anti-*MYCN* siRNA (siMYCN) and Negative control siRNA (Non-target control pool) (siNeg) were ON-TARGETplus siRNA (Dharmacon, Cambridge, UK) were used in this study. The sequence of siMYCN sense strand is: 5'-CAGCAGUUGC UAAAGAAA UU-3', while the antisense strand was 5'-UUUUCUUUAGCAACUGCUGUU-3'.

siRNA transfections

Prior to transfection, NB cells were seeded at 8×10^4 cells per well in 24-well plates in complete media without Penicillin/Streptomycin and incubated overnight in an incubator at 37 °C in 5% CO₂. The confluency reached approximately 50% the next day. SiMYCN (custom) /siNeg (5-50 μM) (ON-TARGETplus siRNA, Dharmacon, Cambridge, UK) was mixed with Lipofectamine RNAiMAX (RNAiMAX; Thermo Fisher Scientific, Northumberland, UK) at a 1:1 volume ratio in OptiMEM (Thermo Fisher Scientific, Northumberland, UK). After 10 minutes incubation, the nanocomplexes were added to cells in complete culture media, and the plates were centrifuged at 400 x g for 5 minutes immediately. The cells were incubated for 48 hours at 37 °C in 5% CO₂.

Quantitative real time RT-PCR (qRT-PCR)

Total RNA was extracted using a RNeasy mini kit (Qiagen, Manchester, UK) then 10-50 ng total RNA were mixed with the SensiFAST Probe Hi-ROX one-step kit (Bioline, London, UK) according to the company's instruction. TaqMan probes (Thermo Fisher Scientific, Northumberland, UK) used in this study were: Human *ActB* (Assay ID: Hs01060665_g1), Human *MYCN* (Hs00232074_m1), Human *NTRK1* (Hs01021011_m1). The cycles were performed in the Bio-Rad 96 PCR machine and Ct values were obtained using Bio-Rad CFX manager (Bio-Rad Laboratories, Hemel Hempstead, UK). The silencing efficiency was calculated by Delta-Delta Ct analysis.

Differentiation in SK-N-BE(2) cells

SK-N-BE(2) cells were seeded at 5×10^4 cells per well in 12-well tissue culture plates (Nunc, Thermo Fisher Scientific, Northumberland, UK) and were incubated at 37 °C in 5% CO₂. Cell images were taken under bright field using an Olympus IX70 microscope with a Canon DS126191 camera attached. 5 images were chosen randomly from each condition, and the experiment was performed twice. The neurite length was measured using Fiji Image J (Supplementary data; Materials and Methods) with extended neurites defined as projections longer than the cell itself as SK-N-BE(2) cells naturally have short neurites (arrow in untransfected control in Fig. 4a). Neurites were traced using Straight>Freehand Line function and the lengths were measured in pixels. To smooth the freehand-drawn lines and interpolate pixel coordinates, Interpolate (Edit>Selection>Interpolate) was used with interval=10 and 'smooth'. The macro commands (below) were run every time a freehand line was drawn. Cell area was measured using the polygon selections function.

1. run("Interpolate", "interval=10 smooth");
2. roiManager("add")

Proliferation assay

Resazurin method: Cells were seeded in a 96-well black plate at a concentration of 3×10^3 in 200 μ L complete media per well and incubated overnight. The transfected/treated cells were incubated in an incubator under 5% CO₂ at 37 °C for 6 days. 20 μ L 0.15 mg/mL Resazurin (Sigma-Aldrich, Dorset, UK) in PBS were added into each well, and incubated for 3 hours in an incubator. Fluorescence was measured

using a 540 nm excitation/590 nm emission wavelength by a FLUOstar Optima plate reader (BMG Labtech, Aylesbury, UK).

CCK-8 method: Cells were seeded in a 96-well plate at a concentration of 6×10^3 in 200 μ L of complete media per well and incubated overnight. 10 μ L Cell counting kit-8 reagent (Sigma-Aldrich, Dorset, UK) were added into each well, and incubated for 3.5 hours in an incubator. The absorbance at 450 nm was measured using the FLUOstar Optima plate reader (BMG Labtech, Aylesbury, UK).

Cell Viability assay

Cells were seeded at 1.5×10^4 cells per well in 96-well plates, and were incubated in an incubator under 5% CO₂ at 37 °C overnight. At 24 hours after transfection, the growth medium was changed and MTS reagent (CellTiter 96 Aqueous One Solution Cell Proliferation Assay, Promega, Wisconsin, USA) was added. Cells were incubated for a further 2 hours at 37 °C, then the absorbance at 492 nm was measured using the FLUOstar Optima plate reader (BMG Labtech, Aylesbury, UK).

Immunoblotting

The total protein of transfected cells was extracted with NP40 Cell Extraction buffer and the concentrations of protein in lysates quantified using a bicinchoninic acid (BCA) kit (Thermo Fisher Scientific, Northumberland, UK). Up to 10 μ g of total protein was mixed with 4x loading dye buffer supplemented with 10x DDT. It was boiled at 100 °C for 5 minutes then electrophoresed on 4-12% Bis-Tris Nupage gel (Thermo Fisher Scientific, Northumberland, UK) in MOPS buffer (Thermo Fisher Scientific, Northumberland, UK) at 150 V for 1 hour. The protein bands were transferred to Polyvinylidene Difluoride (PVDF) membranes (Millipore, Watford, UK) in transfer buffer (25 mM Tris, 192 mM glycine, 20% Methanol) using Bio-Rad Mini Trans-Blot tank (Bio-Rad Laboratories, Hemel Hempstead, UK) at 100 V for 1.5 hours. PVDF membranes were then blocked with 10% dried milk in TBST (50 mM Tris-base pH 7.5, 150 mM NaCl, 0.2% Tween-20) for 1 hour then probed and incubated with anti-MYCN (B8.4.B, 1:8000, Santa Cruz, California, USA) or anti-pan Trk (B-3, 1:2000, Santa Cruz, California, USA) antibodies in 10% dried milk TBST overnight while anti- β -Actin antibody (1:10,000, Sigma-Aldrich, Dorset, UK), was incubated for 1 hour. The

membranes were then washed three times with TBST and incubated with horseradish peroxidase-conjugated secondary antibody (1:10,000, Deko, Glostrup Municipality, Denmark) in 10% dried milk TBST buffer. They were then washed with TBST again, and the protein bands were detected using the ECL chemiluminescence-based detection kit (Bio-Rad, California, USA), and visualised in the UVChemi chemiluminescence detection apparatus (UV Chemistry Co, California, USA). The experiments were repeated three times in SK-N-BE(2) transfected with siRNA and twice in Kelly cells transfected with siRNA. SK-N-BE(2) and Kelly treated with RA were repeated twice.

Statistical Analysis

The error bars indicate the mean \pm standard deviation and results were analysed using a two-tailed, unpaired Student t-test unless mentioned otherwise, in which case a one-way ANOVA was performed. Probability values $p < 0.05$ were indicated as *, $p < 0.01$ were indicated as ** and $p < 0.001$ were indicated as ***.

RESULTS

Cytotoxicity assay

We first investigated the potential toxicity of transfections with *MYCN* mRNA (siMYCN) and scrambled siRNA (siNeg) using RNAiMAX at 50 nM and 10 nM in SK-N-BE(2) cells (Fig. 1). There was no apparent toxicity of 10 nM siMYCN or 10 nM siNeg compared to untransfected control cells ($p=0.9$ and 0.2 , respectively) while 50 nM siMYCN and 50 nM siNeg displayed significant toxicity ($p<0.001$), with only 36% and 42% of cells remaining alive. Thus, siRNA concentrations in RNAiMAX formulations of 20 nM, 10 nM and 5 nM were chosen for the conditions in this study.

MYCN silencing by siRNA in NB cell lines

siMYCN was chosen from three candidate siRNAs targeting *MYCN* mRNA (Fig. S1a, b). *MYCN* mRNA/N-Myc expression levels in three NB cell lines SK-N-BE(2), Kelly and SK-N-SH were investigated using qRT-PCR and immunoblotting respectively. The *MYCN* mRNA and N-Myc expression levels were elevated at 500-2000-fold, and 4-fold to 20-fold respectively, in the *MYCN*-amplified NB cell lines SK-N-BE(2) and Kelly (Fig. S2a, b). Transfections of siMYCN (5-20 nM) using RNAiMAX were performed in the NB cell lines and *MYCN* silencing efficiencies were determined among the different cell lines by qRT-PCR (Fig. 2a, $n=3$). In SK-N-BE(2), the maximal silencing of 38% relative to siNeg was achieved at 20 nM siMYCN with statistical difference between siMYCN and siNeg also observed at 10 nM ($p<0.05$) but not at the 5 nM dose. In Kelly cells, the maximal silencing was also achieved with 20 nM siMYCN (51%), relative to siNeg control ($p<0.05$). In SK-N-SH cells, 20 nM, 10 nM and 5 nM doses of siMYCN achieved similar silencing efficiencies of approximately 55%. although 5 nM siMYCN silencing was not significant compared to 5 nM siNeg ($p=0.07$) while those at 20 nM and 10 nM were ($p<0.01$ and 0.001 , respectively).

Expression of *NTRK1*, which encodes TrkA, a neuronal differentiation marker, was quantified by qRT-PCR in SK-N-BE(2) and Kelly cells, 48 hours after siMYCN transfections (Fig. 2b) to assess the induction of a downstream differentiation marker after *MYCN* silencing. TrkA receptor is expressed on neuronal cells and binds neuron growth factor (NGF) with high affinity inducing differentiation. TrkA expression is

upregulated by N-Myc down-regulation [13], [34, 35]. In SK-N-BE(2) cells, *NTRK1* was upregulated by siMYCN-mediated *MYCN* silencing by 2.0- to 3.3-fold compared to siNeg (Fig. 2b) ($p < 0.05$ for all concentrations) while in Kelly cells, *NTRK1* was upregulated 1.3- to 4.4-fold over siNeg treated cells ($p < 0.05$ for each concentration) (Fig. 2b, $n=3$).

Comparison of *MYCN* silencing and Trk upregulation by siMYCN and retinoic acid at the protein level

We then investigated the effects of siMYCN-mediated *MYCN* silencing on protein expression by Western blot analysis. SK-N-BE(2) and Kelly cells were transfected with siMYCN or siNeg at 20 nM, 10 nM and 5 nM and were harvested 72h after transfection. Western blots were probed with antibodies to N-Myc, pan-Trk, which stains for TrkA, B and C, and β -actin as a house keeping gene (Fig. 3a, b). The dose-response of N-Myc and Trk to all-*trans* retinoic acid (RA) of SK-N-BE(2) and Kelly cell lines was also assessed in a range of concentrations up to 25 μ M. In previous studies, NB cells were treated with RA *in vitro* up to 10 μ M [36, 37], while the 5-10 μ M RA doses are equivalent to the those used in clinical trials by oral administration to NB patients [38, 39] and so RA doses in this concentration range were used. The intensity of all bands from staining for N-Myc, pan-Trk and β -actin was measured using Image J, and the values of N-Myc and pan-Trk were normalised to β -actin and to the untransfected control cells (untransfected control = 1). The relative expression level of each protein is shown under the respective band (Fig. 3). The experiments were repeated three or two times and the average values of the normalised N-Myc and Trk are shown (Fig. 3).

siMYCN reduced N-Myc by up to 95% in SK-N-BE(2) and up to 84% in Kelly cells (Fig 3a, b). Furthermore, siMYCN-mediated N-Myc silencing upregulated the pan-Trk expression level by up to 2.4-fold in SK-N-BE(2) and 6.7-fold in Kelly cells, compared with the respective untransfected cells while siNeg had no significant effects on protein expression. SiRNA-mediated N-Myc reduction was consistent among the three repeated experiments of SK-N-BE(2) and between the twice repeated experiments with Kelly cells. The 5 μ M, 10 μ M RA and 25 μ M RA reduced N-Myc levels by 39% and 32% and 66% respectively in SK-N-BE(2) while N-myc was reduced by 82 %, in Kelly

cells with 5 μM RA with a slightly improved reduction of 92% with 25 μM RA (Fig. 3c, d). Furthermore, RA upregulated Trk expression levels in both SK-N-BE(2) and Kelly (Fig. 3c, d).

Thus, N-Myc protein with 25 μM RA (66%), was equivalent to that of 5 nM siMYCN (73%) in SK-N-BE(2), whilst in Kelly cells N-Myc protein reduction with 10 μM RA (88%) similar to that of 20 nM siMYCN (84%). 25 μM RA achieved the highest Trk expression level in SK-N-BE(2) (7-fold increase) while siMYCN did not achieve this level with a maximum of 2.3-fold increase of Trk. 12.5 μM RA treatment of Kelly cells led to a 5.8 -fold increase in Trk similar to 5nM siMYCN (6.5-fold increase).

In SK-N-BE(2) cells N-myc and Trk levels were fairly constant at all three doses of siMYCN. Kelly cells showed a shallow dose response to siMYCN of reducing N-Myc but this did not correlate with a Trk dose response. Only with Kelly cells was there an apparent correlation of reduced N-myc with elevated Trk in response to an increasing RA concentration.

Differentiation of SK-N-BE(2) cells by siMYCN

We then quantified neurite elongation as an index of differentiation after treatment with siMYCN or RA [8], determining the length and number of the neurites. SK-N-BE(2) transfection with siMYCN (5 nM 10 nM and 20 nM) (induced significant neurite elongation with extended, inter-connecting neurites while cells also became elongated and thinner in appearance, all characteristics of differentiated cells (Fig. 4a, S3). SK-N-BE(2) cells tend to grow in clumps making counting of cells problematic and so, to quantify neurites, the total neurite length value per image was normalised to the total cell area rather than cell number. The experiment was performed twice and five images were analysed in each experiment.

The neurite extensions appeared from 48 hours after transfection, with a total neurite length induced by siMYCN of approximately 0.015-0.025 $\mu\text{m}/\mu\text{m}^2$ cell area (Fig. 5a). The length of neurites transfected with 20 nM, 10 nM and 5 nM siMYCN at day 6 was increased from 48 hours by around 0.03 $\mu\text{m}/\mu\text{m}^2$ cell area and each was significantly different from siNeg controls at the same concentration ($p < 0.001$). The increased neurite length was almost the same at the three different concentrations of siMYCN

(0.033-0.035 $\mu\text{m}/\mu\text{m}^2$ cell area) (Fig. 5a). However, although their length increased, the number of neurites did not change between days 2 and 6 (Fig. 5b). Transfections with siNeg had no effect on neurite length or number at day 2 and day 6. These results suggest that siMYCN treatment induces differentiation in SK-N-B-(BE2) NB cells.

Four different cell lines: SK-N-BE(2), Kelly, LAN-5 that all have *MYCN* amplification and SK-N-SH, which is not *MYCN* amplified, were then treated with 10 μM RA (Fig. 4b). In SK-N-SH cell cultures, where there are normally two types of cells, neuronal and Schwann cell, the morphology of the Schwann-type cells became flatter after the RA treatment (Fig. 4b) while extended neurites formed networks and connected cells. In LAN-5, the extended neurites also formed networks among the cells after treatment with RA. On the other hand, SK-N-BE(2) and Kelly cells did not change their appearance significantly and neurite networks were not induced. Therefore, these results suggest that, despite reduced N-Myc and elevated Trk protein, Kelly and SK-N-BE(2) cells are resistant to treatment with RA.

Suppression of cell viability by siMYCN

We next compared the potential of siMYCN and RA treatment to suppress cellular proliferation. Transfection with 10 nM siMYCN suppressed cell viability over the 3 days, and the cell growth rate was relative to siNeg and untransfected control cells (all $p < 0.05$). In addition, the cell growth rate of SK-N-BE(2) treated with 20 nM siMYCN, reduced the viability, but no significant differences were observed between 5 nM siMYCN and siNeg (Fig. S4).

We then assessed whether there was a beneficial effect of co-treatment of siMYCN and RA. The growth rate was measured using a resazurin assay at 6 days after siMYCN transfection or RA treatment ($n=3$) (Fig. 6b, Table 1). The experiment was performed four times and the values were normalised to untransfected cells. Cell growth rates showed no benefit of the combined siMYCN and RA treatment while RA on its own was also ineffective at retarding cell proliferation. However, all formulations with siMYCN were effective under all conditions ($p < 0.05$). These results confirm that siMYCN suppresses proliferation of SK-N-BE(2) and, here, show that it does this with

much greater efficacy than RA, and so could be therapeutically beneficial in suppressing cell growth in addition to differentiation in RA-resistant cells.

DISCUSSION

SiRNA therapies, after many years of development [24] have finally begun to realise their potential in developing therapies with the first approved and effective product, Onpattro, a lipid nanoparticle (LNP) siRNA therapy delivered to the liver to treat transthyretin amyloidosis [25]. Delivery to tumours has been investigated extensively, including clinical trials, but so far without an approved product [26-28] but the success of Onpattro has provided fresh stimulus to the siRNA field. MYCN targeted therapies have also been under investigation for more than 20 years, motivated by its contribution to NB tumorigenicity, particularly in MYCN-amplified tumours. As a transcription factor, MYCN is a difficult target for drug development making siRNA an attractive approach. In order to develop siRNA MYCN therapies it is important to understand the functionality of these formulations.

In this paper, we have investigated the potential of *MYCN* silencing by RNAi as a therapy for NB by building on previous studies and further analysing its effects on cell differentiation and proliferation. In particular we have compared the efficacy of siMCYN in cell resistant to retinoic acid, an established treatment for NB but for which resistance can become a problem [40]. Over-expressed N-Myc induces proliferation, which is one of the characteristics of tumorigenesis in *MYCN*-amplified NB, and also suppresses differentiation initiated by neuron growth factor (NGF) [13]. N-Myc downregulates TrkA expression by forming a repression complex with the transcription factors SP1 and MIZ1 at the core promoters of TrkA, and the complex then recruits the histone deacetylase HDAC1 to suppress transcription [41]. TrkA receptor, activated by NGF ligand, stimulates differentiation in normal cells *in vitro* [42] while lack of TrkA expression from overexpressed N-Myc correlates to poor prognosis in NB [43].

There is increasing evidence that MYCN is a suitable target for NBN therapies. Recent studies have shown that overexpression of N-Myc inhibits TGFB1, which is activated by RA and a ligand of transforming growth factor beta (TGF- β) signalling [44]. In addition, overexpression of N-Myc inhibits TGFB1, which is required as a differentiation modulator [44]. The Wnt/ β -catenin signalling pathway is crucial for cell proliferation, differentiation, apoptosis, polarity and pluripotency and is thus a target for NB [45, 46]. N-Myc suppression down-regulates Wnt/ β -catenin signalling [46] while activation of Wnt/ β -catenin signalling by the transcription factor HIF1/2 α , leads to an undifferentiated state in neuroblastoma [47]. Thus, HIF inhibition induces differentiation in NB cells by RA by blocking the Wnt/ β -catenin pathway [47]. Similarly, the combination of Wnt/ β -catenin signalling inhibition and RA treatment significantly reduces NB cell viability and forces surviving cells to differentiate [48].

RA targets the retinoic acid receptor/retinoic X receptor (RAR/RXR) in normal neuronal cells, and induces TrkA upregulation and differentiation in both *MYCN*-amplified and non-*MYCN* amplified tumour cells [13] and so RA has been used as a therapy for high-risk neuroblastoma for controlling minimal residue after high-dose chemotherapy [37]. However, some NB cells develop resistance to RA, such as the NB cell line SK-N-BE(2), which may result from defective retinoid signalling downstream of TrkA [49]. RA catabolism by members of the cytochrome P450 family, such as CYP26 enzymes which specifically inhibit RA may be involved in resistance in NB [36, 50, 51].

A large number of markers have been identified associated with neuroblastoma differentiation [8] and here we found that TrkA was particularly useful to monitor differentiation of SK-N-BE(2) cells after siMYCN treatment. TrkA mRNA expression was shown to be upregulated while Trk proteins were shown to be upregulated by a panTrk antibody that also recognises TrkB and Trk C as well as TrkA. This antibody worked particularly well and along with the mRNA data provides strong evidence of upregulation of Trk differentiation markers, although it would be interesting to dissect upregulation of each Trk in future studies. protein levels in SK-N-BE(2), inducing extensive neurite elongation in *MYCN*-amplified, p53-deficient SK-N-BE(2) cells, and suppressing cellular proliferation. In comparison, treatment of SK-N-BE(2) with 10 μ M RA in this study, reduced N-Myc by 30%, similar to previous reports [49]. This level of N-Myc reduction was similar to that with siMYCN and led to upregulated Trk expression, but no neurites or other significant differentiation-related, morphological

changes were seen, suggesting that these cells are resistant to RA treatment[49]. In contrast, RA treatment in SK-N-SH and LAN-5 cells induced neurite formation and morphological changes indicating this treatment was effective in these NB cell types. RA treatment in Kelly cells induced N-Myc silencing and enhanced Trk expression but otherwise had no effect on the morphology.

SK-N-BE(2) cells are resistant toward, not only RA, but also other anti-cancer drugs such as doxorubicin, etoposide, cisplatin, carboplatin and melphalan that depend on the p53 pathway as this cell line was established from cells isolated from a patient after several sessions of chemotherapy and radiotherapy [52, 53]. Our data suggests that siMYCN might be a promising therapy in cases of NB with resistance towards RA and other drugs that rely on the p53 pathway to induce apoptosis or differentiation, as observed with SK-N-BE(2) cells.

In this study, in SK-N-BE(2) cells, silencing of *MYCN* was siRNA dose-dependent and this led to a dose-related increase of *NTRK1* mRNA, although this did not lead to elevated Trk protein expression, e.g., 5 nM siMYCN led to a similar level of Trk elevation as 20 nM siMYCN. Likewise, there was no difference in the induction of neurite formation from 5 nM to 20 nM siMYCN indicating that even levels of *MYCN* silencing of 25% - 30% is sufficient to induce differentiation and reduced cell growth.

However, it is important to be aware that not all NB cells respond to N-myc reduction by differentiating. In fact, *MYCN* expression is required for the differentiation of some NB cells [54, 55]. Thus, not all *MYCN*-amplified NB will differentiate on *MYCN* suppression, due to the heterogeneity of neuroblastoma.

In conclusion, we have demonstrated that siRNA-mediated silencing of *MYCN* expression at the mRNA and protein levels, and it induces NTRK1/TrkA upregulation in SK-N-BE(2) and Kelly cells. Importantly, siMYCN transfections significantly trigger neurite elongation, a differentiation marker, on SK-N-BE(2), which has non-functional p53 and has resistance towards RA and drug depending p53-pathway. Therefore, *MYCN* silencing by siRNA may provide a novel therapy for NB with drug resistance. These results will enable us to proceed to *in vivo* studies in murine models of NB, for which we have developed novel siRNA nanoparticle formulations [31, 56].

Conflict of interest

None

Acknowledgements

This work was supported by the National Institute for Health Research Biomedical Research Centre at Great Ormond Street Hospital for Children NHS Foundation Trust and University College London. We are grateful for the financial support of Dr. Michihiro Maeshima M.D.

References

1. Huang M, WA Weiss (2013). Neuroblastoma and MYCN. *Cold Spring Harb Perspect Med* 3:a014415.
2. Kang JH, PG Rychahou, TA Ishola, J Qiao, BM Evers, DH Chung (2006). MYCN silencing induces differentiation and apoptosis in human neuroblastoma cells. *Biochem Biophys Res Commun* 351:192-197.
3. Buechner J, C Einvik (2012). N-myc and noncoding RNAs in neuroblastoma. *Mol Cancer Res* 10:1243-1253.
4. Pichler M, GA Calin (2014). Long noncoding RNA in neuroblastoma: new light on the (old) N-Myc story. *J Natl Cancer Inst* 106(7), dju150.
5. Maris JM, MD Hogarty, R Bagatell, SL Cohn (2007). Neuroblastoma. *Lancet* 369:2106-2120.
6. Murphy JM, MP La Quaglia (2014). Advances in the surgical treatment of neuroblastoma: a review. *Eur J Pediatr Surg* 24:450-456.
7. Cheung NK, MA Dyer (2013). Neuroblastoma: developmental biology, cancer genomics and immunotherapy. *Nat Rev Cancer* 13:397-411.
8. Dzieran J, A Rodriguez Garcia, UK Westermarck, AB Henley, E Eyre Sanchez, C Trager, HJ Johansson, J Lehtio, M Arsenian-Henriksson (2018). MYCN-amplified neuroblastoma maintains an aggressive and undifferentiated phenotype by deregulation of estrogen and NGF signaling. *Proc Natl Acad Sci U S A* 115:E1229-E1238.
9. Clark O, S Daga, AW Stoker (2013). Tyrosine phosphatase inhibitors combined with retinoic acid can enhance differentiation of neuroblastoma cells and trigger ERK- and AKT-dependent, p53-independent senescence. *Cancer Lett* 328:44-54.
10. Yu M, M Ohira, Y Li, H Niizuma, ML Oo, Y Zhu, T Ozaki, E Isogai, Y Nakamura, T Koda, S Oba, B Yu, A Nakagawara (2009). High expression of ncRAN, a novel non-coding RNA mapped to chromosome 17q25.1, is associated with poor prognosis in neuroblastoma. *Int J Oncol* 34:931-938.
11. Barone G, J Anderson, AD Pearson, K Petrie, L Chesler (2013). New strategies in neuroblastoma: Therapeutic targeting of MYCN and ALK. *Clin Cancer Res* 19:5814-5821.

12. Ploessl C, A Pan, KT Maples, DK Lowe (2016). Dinutuximab: An Anti-GD2 Monoclonal Antibody for High-Risk Neuroblastoma. *Ann Pharmacother* 50:416-422.
13. Westermark UK, M Wilhelm, A Frenzel, MA Henriksson (2011). The MYCN oncogene and differentiation in neuroblastoma. *Semin Cancer Biol* 21:256-266.
14. Beltran H (2014). The N-myc Oncogene: Maximizing its Targets, Regulation, and Therapeutic Potential. *Mol Cancer Res* 12:815-822.
15. Duffy DJ, A Krstic, M Halasz, T Schwarzl, D Fey, K Iljin, JP Mehta, K Killick, J Whilde, B Turriziani, S Haapa-Paananen, V Fey, M Fischer, F Westermann, KO Henrich, S Bannert, DG Higgins, W Kolch (2015). Integrative omics reveals MYCN as a global suppressor of cellular signalling and enables network-based therapeutic target discovery in neuroblastoma. *Oncotarget* 6:43182-43201.
16. Sabo A, TR Kress, M Pelizzola, S de Pretis, MM Gorski, A Tesi, MJ Morelli, P Bora, M Doni, A Verrecchia, C Tonelli, G Faga, V Bianchi, A Ronchi, D Low, H Muller, E Guccione, S Campaner, B Amati (2014). Selective transcriptional regulation by Myc in cellular growth control and lymphomagenesis. *Nature* 511:488-492.
17. Walz S, F Lorenzin, J Morton, KE Wiese, B von Eyss, S Herold, L Rycak, H Dumay-Odelot, S Karim, M Bartkuhn, F Roels, T Wustefeld, M Fischer, M Teichmann, L Zender, CL Wei, O Sansom, E Wolf, M Eilers (2014). Activation and repression by oncogenic MYC shape tumour-specific gene expression profiles. *Nature* 511:483-487.
18. He S, Z Liu, DY Oh, CJ Thiele (2013). MYCN and the epigenome. *Front Oncol* 3:1.
19. Zimmerman KA, GD Yancopoulos, RG Collum, RK Smith, NE Kohl, KA Denis, MM Nau, ON Witte, D Toran-Allerand, CE Gee, et al. (1986). Differential expression of myc family genes during murine development. *Nature* 319:780-783.
20. Zhu Q, C Feng, W Liao, Y Zhang, S Tang (2013). Target delivery of MYCN siRNA by folate-nanoliposomes delivery system in a metastatic neuroblastoma model. *Cancer Cell Int* 13:65. doi.org/10.1186/1475-2867-13-65
21. Feng C, TY Wang, RH Tang, JW Wang, H Long, XN Gao, SQ Tang (2010). Silencing of the MYCN gene by siRNA delivered by folate receptor-targeted liposomes in LA-N-5 cells. *Pediatric Surgery International* 26:1185-1191.
22. Nara K, T Kusafuka, A Yoneda, T Oue, S Sangkhathat, M Fukuzawa (2007). Silencing of MYCN by RNA interference induces growth inhibition, apoptotic activity and cell differentiation in a neuroblastoma cell line with MYCN amplification. *Int J Oncol* 30:1189-1196.

23. Burkhart CA, AJ Cheng, J Madafiglio, M Kavallaris, M Mili, GM Marshall, WA Weiss, LM Khachigian, MD Norris, M Haber (2003). Effects of MYCN antisense oligonucleotide administration on tumorigenesis in a murine model of neuroblastoma. *J Natl Cancer Inst* 95:1394-1403.
24. Fire A, S Xu, MK Montgomery, SA Kostas, SE Driver, CC Mello (1998). Potent and specific genetic interference by double-stranded RNA in *Caenorhabditis elegans*. *Nature* 391:806-811.
25. Adams D, A Gonzalez-Duarte, WD O'Riordan, CC Yang, M Ueda, AV Kristen, I Tournev, HH Schmidt, T Coelho, JL Berk, KP Lin, G Vita, S Attarian, V Plante-Bordeneuve, MM Mezei, JM Campistol, J Buades, TH Brannagan, 3rd, BJ Kim, J Oh, Y Parman, Y Sekijima, PN Hawkins, SD Solomon, M Polydefkis, PJ Dyck, PJ Gandhi, S Goyal, J Chen, AL Strahs, SV Nochur, MT Sweetser, PP Garg, AK Vaishnav, JA Gollob, OB Suhr (2018). Patisiran, an RNAi Therapeutic, for Hereditary Transthyretin Amyloidosis. *N Engl J Med* 379:11-21.
26. Lei Y, L Tang, Y Xie, Y Xianyu, L Zhang, P Wang, Y Hamada, K Jiang, W Zheng, X Jiang (2017). Gold nanoclusters-assisted delivery of NGF siRNA for effective treatment of pancreatic cancer. *Nat Commun* 8:15130.
27. Zhou J, Y Wu, C Wang, Q Cheng, S Han, X Wang, J Zhang, L Deng, D Zhao, L Du, H Cao, Z Liang, Y Huang, A Dong (2016). pH-Sensitive Nanomicelles for High-Efficiency siRNA Delivery in Vitro and in Vivo: An Insight into the Design of Polycations with Robust Cytosolic Release. *Nano Lett* 16:6916-6923.
28. Chakraborty C, AR Sharma, G Sharma, CGP Doss, SS Lee (2017). Therapeutic miRNA and siRNA: Moving from Bench to Clinic as Next Generation Medicine. *Mol Ther Nucleic Acids* 8:132-143.
29. Grosse SM, AD Tagalakakis, MF Mustapa, M Elbs, QH Meng, A Mohammadi, AB Tabor, HC Hailes, SL Hart (2010). Tumor-specific gene transfer with receptor-mediated nanocomplexes modified by polyethylene glycol shielding and endosomally cleavable lipid and peptide linkers. *FASEB J* 24:2301-2313.
30. Tagalakakis AD, SM Grosse, QH Meng, MF Mustapa, A Kwok, SE Salehi, AB Tabor, HC Hailes, SL Hart (2011). Integrin-targeted nanocomplexes for tumour specific delivery and therapy by systemic administration. *Biomaterials* 32:1370-1376.
31. Tagalakakis AD, L He, L Saraiva, KT Gustafsson, SL Hart (2011). Receptor-targeted liposome-peptide nanocomplexes for siRNA delivery. *Biomaterials* 32:6302-6315.

32. Tagalakis AD, DH Lee, AS Bienemann, H Zhou, MM Munye, L Saraiva, D McCarthy, Z Du, CA Vink, R Maeshima, EA White, K Gustafsson, SL Hart (2014). Multifunctional, self-assembling anionic peptide-lipid nanocomplexes for targeted siRNA delivery. *Biomaterials* 35:8406-8415.
33. Tagalakis AD, L Saraiva, D McCarthy, KT Gustafsson, SL Hart (2013). Comparison of nanocomplexes with branched and linear peptides for siRNA delivery. *Biomacromolecules* 14:761-770.
34. Zhang Y, DB Moheban, BR Conway, A Bhattacharyya, RA Segal (2000). Cell surface Trk receptors mediate NGF-induced survival while internalized receptors regulate NGF-induced differentiation. *J Neurosci* 20:5671-5678.
35. Kaplan DR, BL Hempstead, D Martin-Zanca, MV Chao, LF Parada (1991). The trk proto-oncogene product: a signal transducing receptor for nerve growth factor. *Science* 252:554-558.
36. Armstrong JL, GA Taylor, HD Thomas, AV Boddy, CP Redfern, GJ Veal (2007). Molecular targeting of retinoic acid metabolism in neuroblastoma: the role of the CYP26 inhibitor R116010 in vitro and in vivo. *Br J Cancer* 96:1675-1683.
37. Hammerle B, Y Yanez, S Palanca, A Canete, DJ Burks, V Castel, J Font de Mora (2013). Targeting neuroblastoma stem cells with retinoic acid and proteasome inhibitor. *PLoS One* 8:e76761.
38. Reynolds CP, KK Matthay, JG Villablanca, BJ Maurer (2003). Retinoid therapy of high-risk neuroblastoma. *Cancer Lett* 197:185-192.
39. Veal GJ, M Cole, J Errington, AD Pearson, AB Foot, G Whyman, AV Boddy, UPW Group (2007). Pharmacokinetics and metabolism of 13-cis-retinoic acid (isotretinoin) in children with high-risk neuroblastoma - a study of the United Kingdom Children's Cancer Study Group. *Br J Cancer* 96:424-431.
40. Dobrotkova V, P Chlapek, P Mazanek, J Sterba, R Veselska (2018). Traffic lights for retinoids in oncology: molecular markers of retinoid resistance and sensitivity and their use in the management of cancer differentiation therapy. *BMC Cancer* 18:1059.
41. Iraci N, D Diolaiti, A Papa, A Porro, E Valli, S Gherardi, S Herold, M Eilers, R Bernardoni, G Della Valle, G Perini (2011). A SP1/MIZ1/MYCN repression complex recruits HDAC1 at the TRKA and p75NTR promoters and affects neuroblastoma malignancy by inhibiting the cell response to NGF. *Cancer Res* 71:404-412.
42. Eggert A, MA Grotzer, TJ Zuzak, BR Wiewrodt, R Ho, N Ikegaki, GM Brodeur (2001). Resistance to tumor necrosis factor-related apoptosis-inducing ligand

(TRAIL)-induced apoptosis in neuroblastoma cells correlates with a loss of caspase-8 expression. *Cancer Res* 61:1314-1319.

43. Peterson S, E Bogenmann (2004). The RET and TRKA pathways collaborate to regulate neuroblastoma differentiation. *Oncogene* 23:213-225.

44. Duffy DJ, A Krstic, M Halasz, T Schwarzl, A Konietzny, K Iljin, DG Higgins, W Kolch (2017). Retinoic acid and TGF-beta signalling cooperate to overcome MYCN-induced retinoid resistance. *Genome Med* 9:15 doi: 10.1186/s13073-017-0407-3.

45. Szemes M, A Greenhough, K Malik (2019). Wnt Signaling Is a Major Determinant Neuroblastoma Cell Lineages. *Front Mol Neurosci* 12:90
doi10.3389/fnmol.2019.00090

46. Wang Y, S Gao, W Wang, Y Xia, J Liang (2018). Downregulation of NMyC inhibits neuroblastoma cell growth via the Wnt/betacatenin signaling pathway. *Mol Med Rep* 18:377-384.

47. Becker J, J Wilting (2018). WNT signaling, the development of the sympathoadrenal-paraganglionic system and neuroblastoma. *Cell Mol Life Sci* 75:1057-1070.

48. Duffy DJ, A Krstic, T Schwarzl, M Halasz, K Iljin, D Fey, B Haley, J Whilde, S Haapa-Paananen, V Fey, M Fischer, F Westermann, KO Henrich, S Bannert, DG Higgins, W Kolch (2016). Wnt signalling is a bi-directional vulnerability of cancer cells. *Oncotarget* 7:60310-60331.

49. Joshi S, RS Guleria, J Pan, D Dipette, US Singh (2007). Heterogeneity in retinoic acid signaling in neuroblastomas: Role of matrix metalloproteinases in retinoic acid-induced differentiation. *Biochim Biophys Acta* 1772:1093-1102.

50. Chlapek P, V Slavikova, P Mazanek, J Sterba, R Veselska (2018). Why Differentiation Therapy Sometimes Fails: Molecular Mechanisms of Resistance to Retinoids. *Int J Mol Sci* 19. doi:10.3390/ijms19010132.

51. Stevison F, J Jing, S Tripathy, N Isoherranen (2015). Role of Retinoic Acid-Metabolizing Cytochrome P450s, CYP26, in Inflammation and Cancer. *Adv Pharmacol* 74:373-412.

52. Tweddle DA, AJ Malcolm, N Bown, AD Pearson, J Lunec (2001). Evidence for the development of p53 mutations after cytotoxic therapy in a neuroblastoma cell line. *Cancer Res* 61:8-13.

53. Keshelava N, RC Seeger, S Groshen, CP Reynolds (1998). Drug resistance patterns of human neuroblastoma cell lines derived from patients at different phases of therapy. *Cancer Res* 58:5396-5405.
54. Edsjo A, H Nilsson, J Vandesompele, J Karlsson, F Pattyn, LA Culp, F Speleman, S Pahlman (2004). Neuroblastoma cells with overexpressed MYCN retain their capacity to undergo neuronal differentiation. *Lab Invest* 84:406-417.
55. Guglielmi L, C Cinnella, M Nardella, G Maresca, A Valentini, D Mercanti, A Felsani, I D'Agnano (2014). MYCN gene expression is required for the onset of the differentiation programme in neuroblastoma cells. *Cell Death Dis* 5:e1081.
56. Tagalakis AD, DH Lee, AS Bienemann, H Zhou, MM Munye, L Saraiva, D McCarthy, Z Du, CA Vink, R Maeshima, EA White, K Gustafsson, SL Hart (2014). Multifunctional, self-assembling anionic peptide-lipid nanocomplexes for targeted siRNA delivery. *Biomaterials* 35:8406-8415.

Table 1.

The statistics of the resazurin proliferation assay Fig. 6b. One-way ANOVA Bonferroni's multiple comparisons test was performed, * $p < 0.05$, ** $p < 0.01$, *** $p < 0.001$.

Fig. 1 Cytotoxicity assay

Cell viability of SK-N-BE(2) cells treated with 50 nM or 10 nM siMYCN/siNeg were assessed using MTS assay reagent. SiRNA transfections at 50 nM using RNAiMAX were notably toxic while the cell viability of the cells treated with 10 nM siRNAs was almost the same or slightly lower (statistically non-significant) to untransfected negative control cells. ($p < 0.001$ between 50 nM siMYCN and 10 nM siMYCN, and $p < 0.001$ between 50 nM siMYCN and untransfected control cells). In addition, the values between 50 nM siNeg and untransfected control cells were also statistically different with $p < 0.01$ indicating that toxicity was due to the formulation itself rather than MYCN silencing. The intensity was normalised to untransfected negative control cells. (n=5) In the graph each column represents the mean \pm SD, *** $p < 0.001$.

Fig. 2 Relative expression of *MYCN* mRNA and *NTRK1* mRNA in NB cell lines 48 hours after siMYCN transfection quantified by qRT-PCR

a) SK-N-BE(2), Kelly, LAN-5 and SK-N-SH cells were treated with siMYCN and siNeg for 48 hours, and the MYCN mRNA expression level was quantified using qRT-PCR. The values were normalised by the value of siNeg at each concentration. siMYCN silenced MYCN up to 45.9% in SK-N-BE(2), 51.2% in Kelly, 12.5 in LAN-5 and 67.5% in SK-N-SH. All the concentrations of siMYCN significantly reduced *MYCN* mRNA in the three cell lines except LAN-5. (n=3) b) After the transfection, mRNA of *NTRK1* was quantified by qRT-PCR. *NTRK1* was significantly upregulated 2-3-fold in SK-N-

BE(2) and 1.3-4.4-fold in Kelly compared to cells treated with siNeg (n=3). In all the graphs, each column represents the mean \pm SD, *p<0.05, **p<0.01, ***p<0.001.

Fig. 3 Immunoblotting of N-Myc and Trk following siMYCN transfections

The number under the band is the relative expression level calculated from the intensity of the band. a) SK-N-BE(2) and b) Kelly cells, were transfected with siMYCN/siNeg for 3 days, and the samples were probed with anti-N-Myc antibody and anti-Pan-Trk antibody. N-Myc bands appeared between 64 kDa and 51 kDa, and Pan-Trk bands above 97 kDa. The bands were quantified and normalised to untransfected control cells and plotted in charts for N-Myc and Trk and compared by a Student t test (**p<0.01, *p<0.05). siMYCN induced N-Myc reduction and Trk upregulation. c, d) Comparison of the effects on N-Myc and Trk expressions of treatment with RA in c) SK-N-BE(2) and d) Kelly shown in immunoblots and quantified in charts. Two separate blots were performed and quantified but statistical analysis was not possible.

Fig. 4 Cell morphology changes after siMYCN transfection or retinoic acid treatment

a) SK-N-BE(2) cells were transfected with siMYCN/siNeg and incubated for 6 days. The morphology was altered by transfection relative to controls, with the formation of elongated neurites (arrows in 10 nM siMYCN) and the presence of rounder and smaller cell bodies. The scale bar represents 100 μ m. b) SK-N-SH, LAN-5, SK-N-BE(2) and Kelly cells were treated with 5 or 10 μ M RA for 48 hours. RA induced neurite elongation in SK-N-SH and LAN-5, while SK-N-BE(2) and Kelly cells did not respond significantly with respect to their morphology. The scale bar represent 100 μ m.

Fig. 5 Quantification of neurites after siMYCN transfection of SK-N-BE(2) cells

siMYCN significantly induced differentiation in SK-N-BE(2) (n=10), and there were significant differences in a) the neurite length and b) the number of the neurites

between siMYCN and siNeg. The neurite length in day 6 was longer than that in day 2 while the number of the neurite were almost the same during the 4 days. In all the graphs each column represents the mean \pm SD, * p <0.05, ** p <0.01, *** p <0.001.

Fig. 6 Analysis of cell viability after siMYCN treatment in SK-N-BE(2) cells

a) SK-N-BE(2) cells were treated with 10nM siMYCN, and the cell growth rates were measured using the CCK-8 assay reagent at 4 time points. 10nM siMYCN remarkably reduced the growth rate during the 3 days. (n=3) Each dot represents the mean, and error bar is standard deviation.* p <0.05, ** p <0.01, *** p <0.001. b) SK-K-BE(2) cells transfected with 10 nM siMYCN and siNeg with/without DMSO or treated with 5 μ M RA. The proliferation rate were measured using resazurin in PBS at Day 6 time point. Each column represents the mean, and the error bar is standard deviation. Two-way ANOVA Bonferroni's multiple comparisons test was performed (Table 1), * p <0.05, ** p <0.01, *** p <0.001.

Fig1

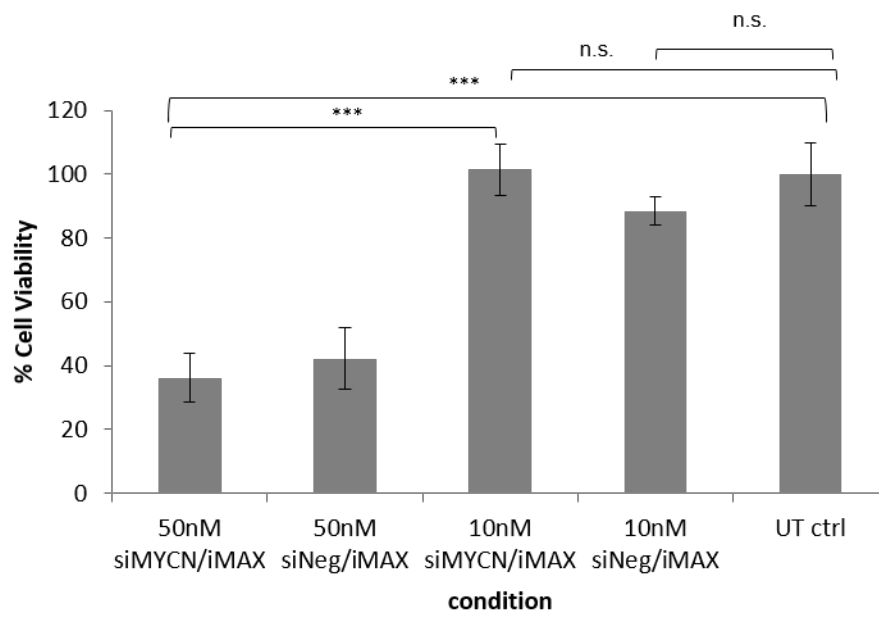
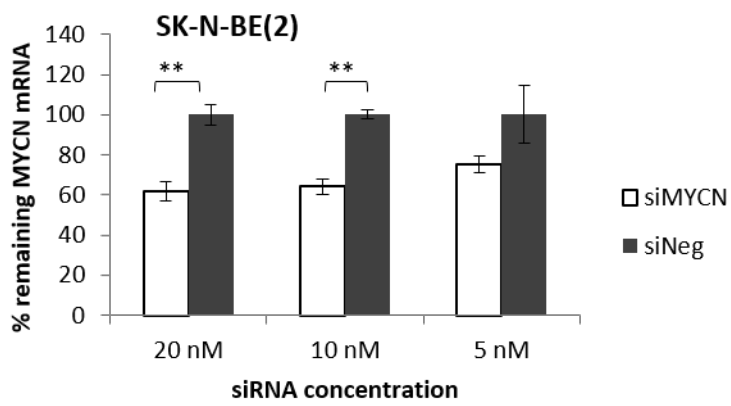
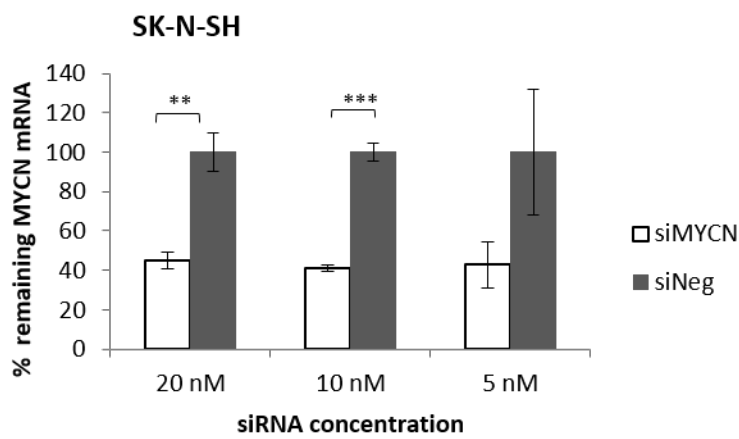
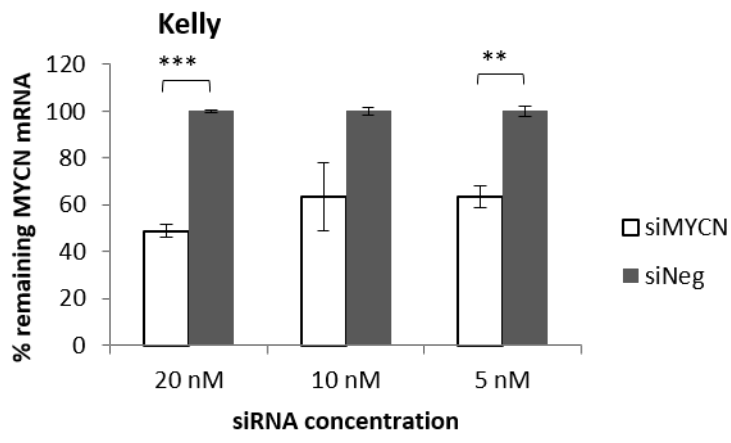


Fig. 2



a)



b)

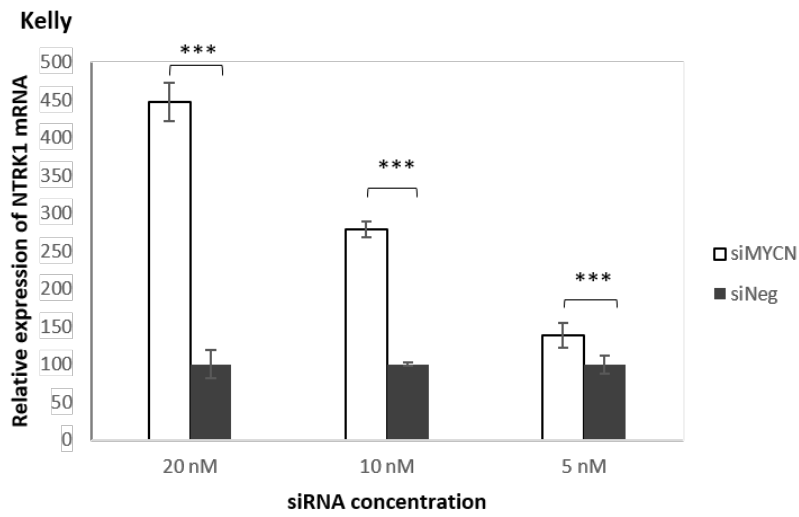
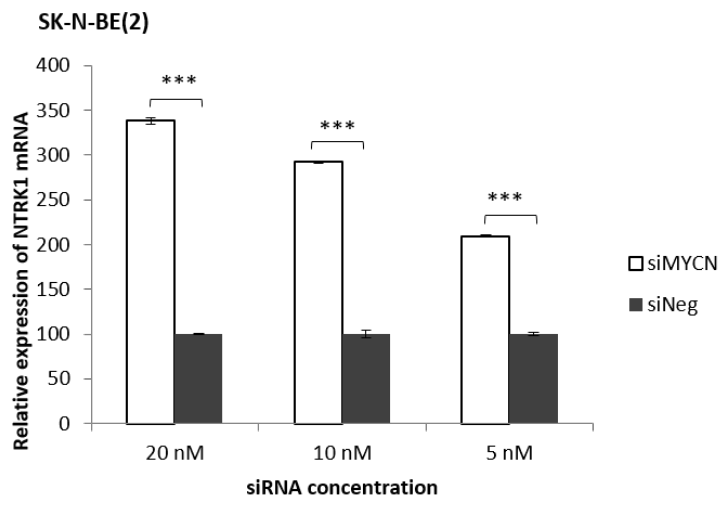
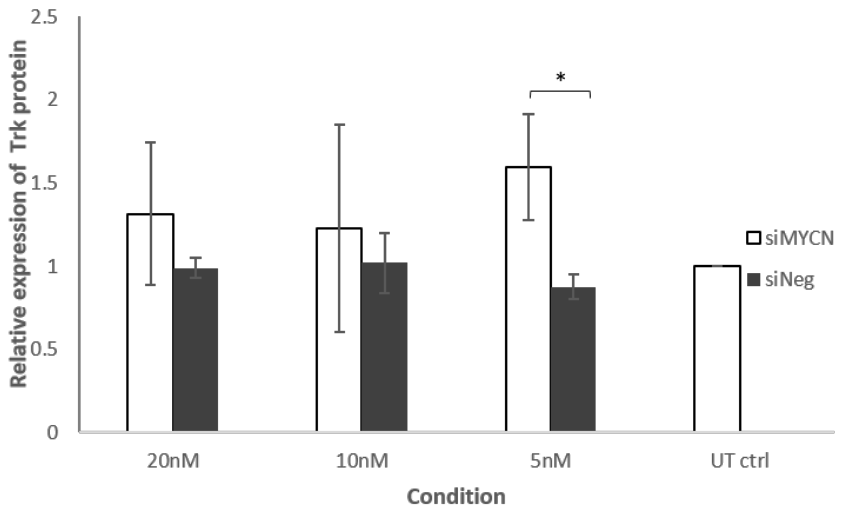
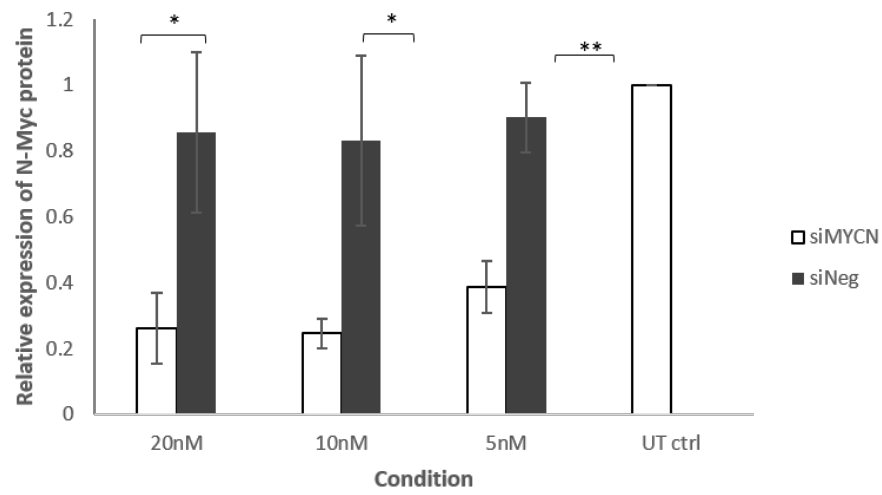
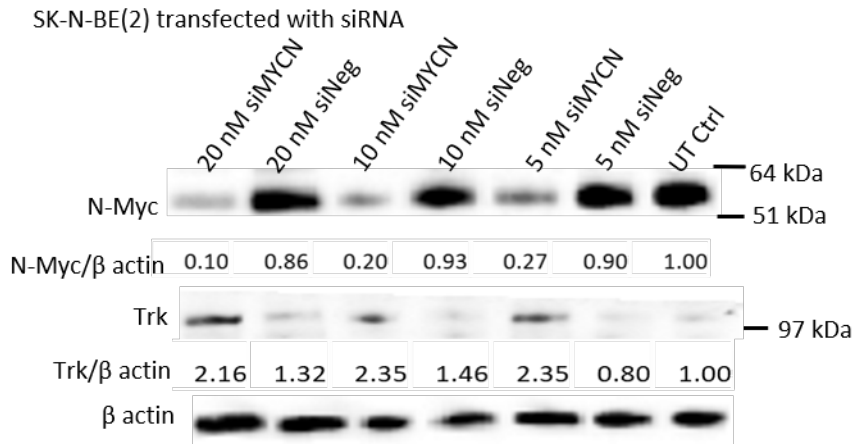


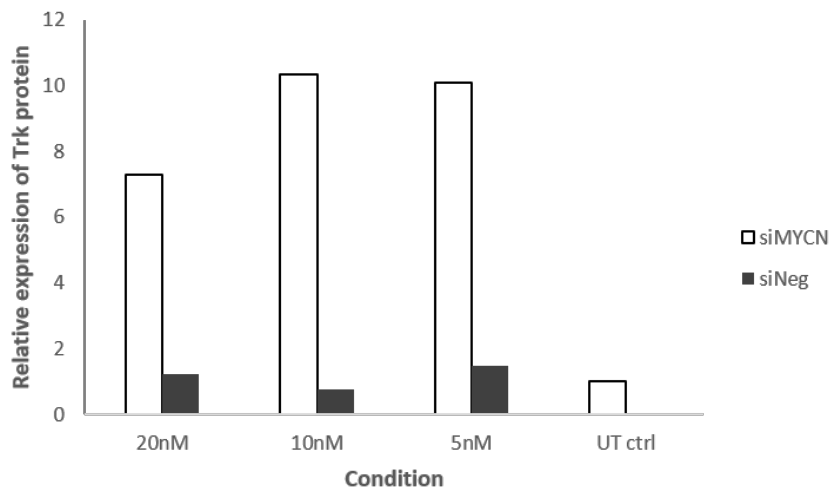
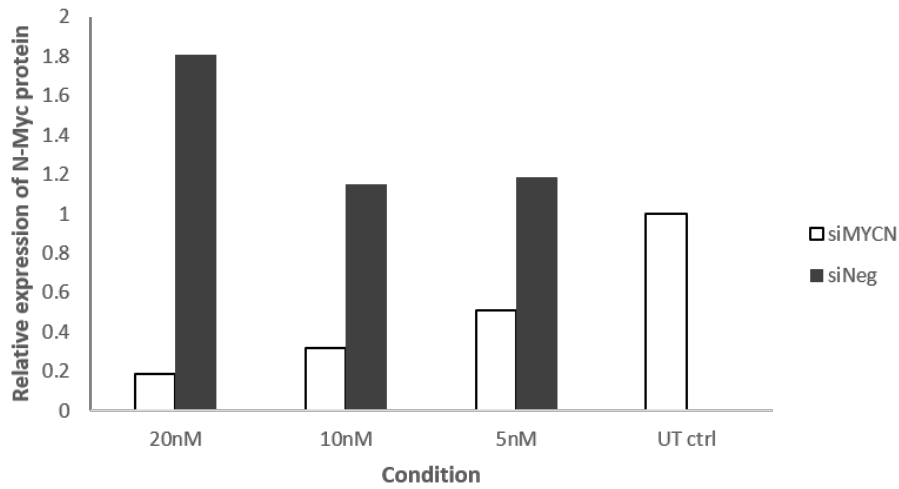
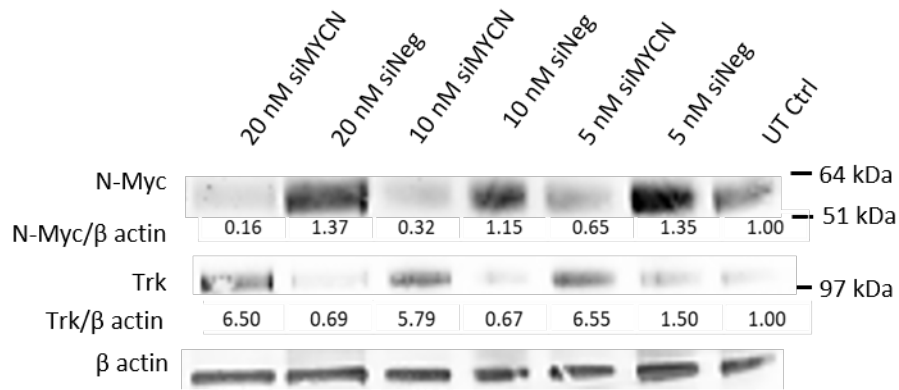
Fig. 3

a)

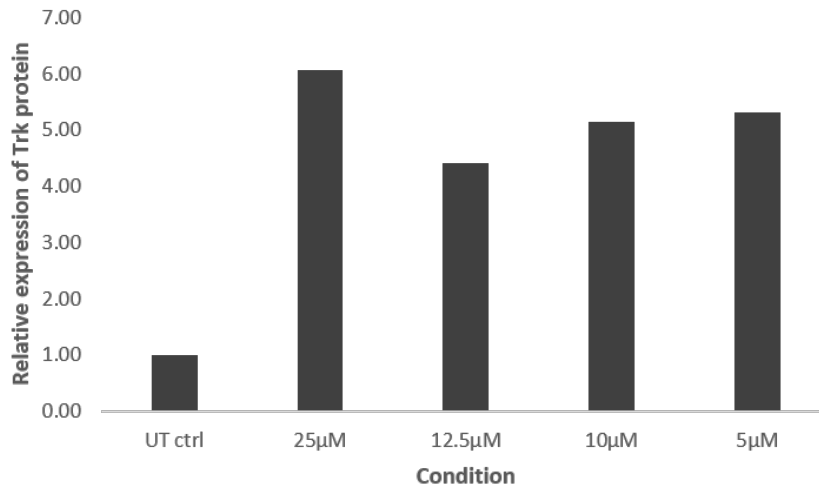
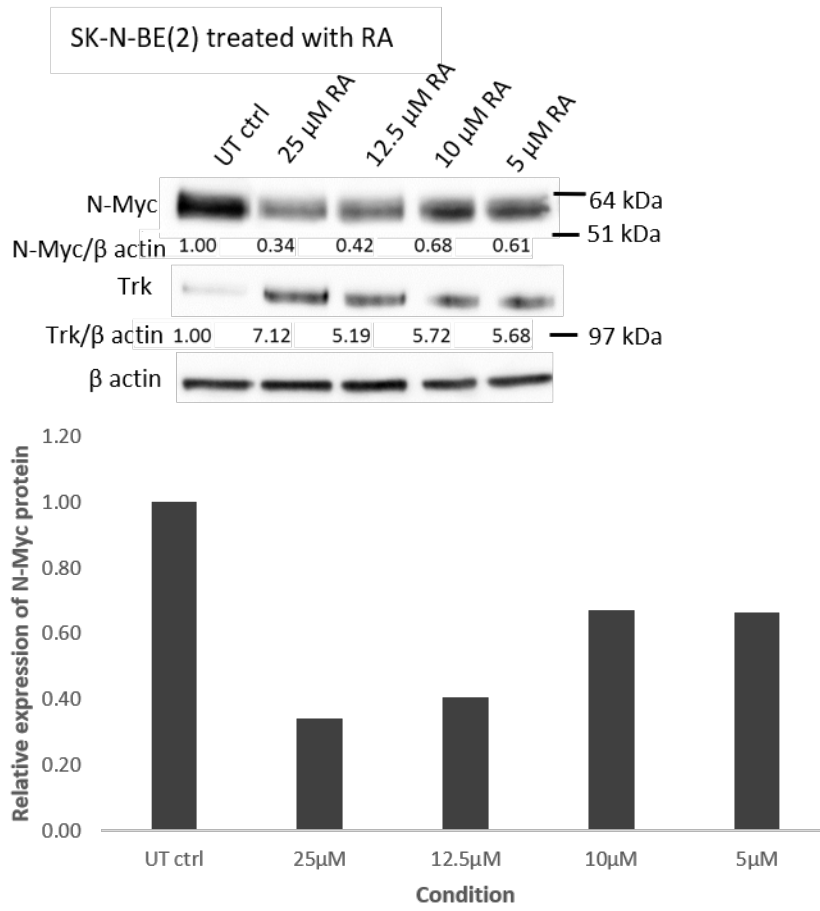


b)

Kelly transfected with siRNA



c)



d)

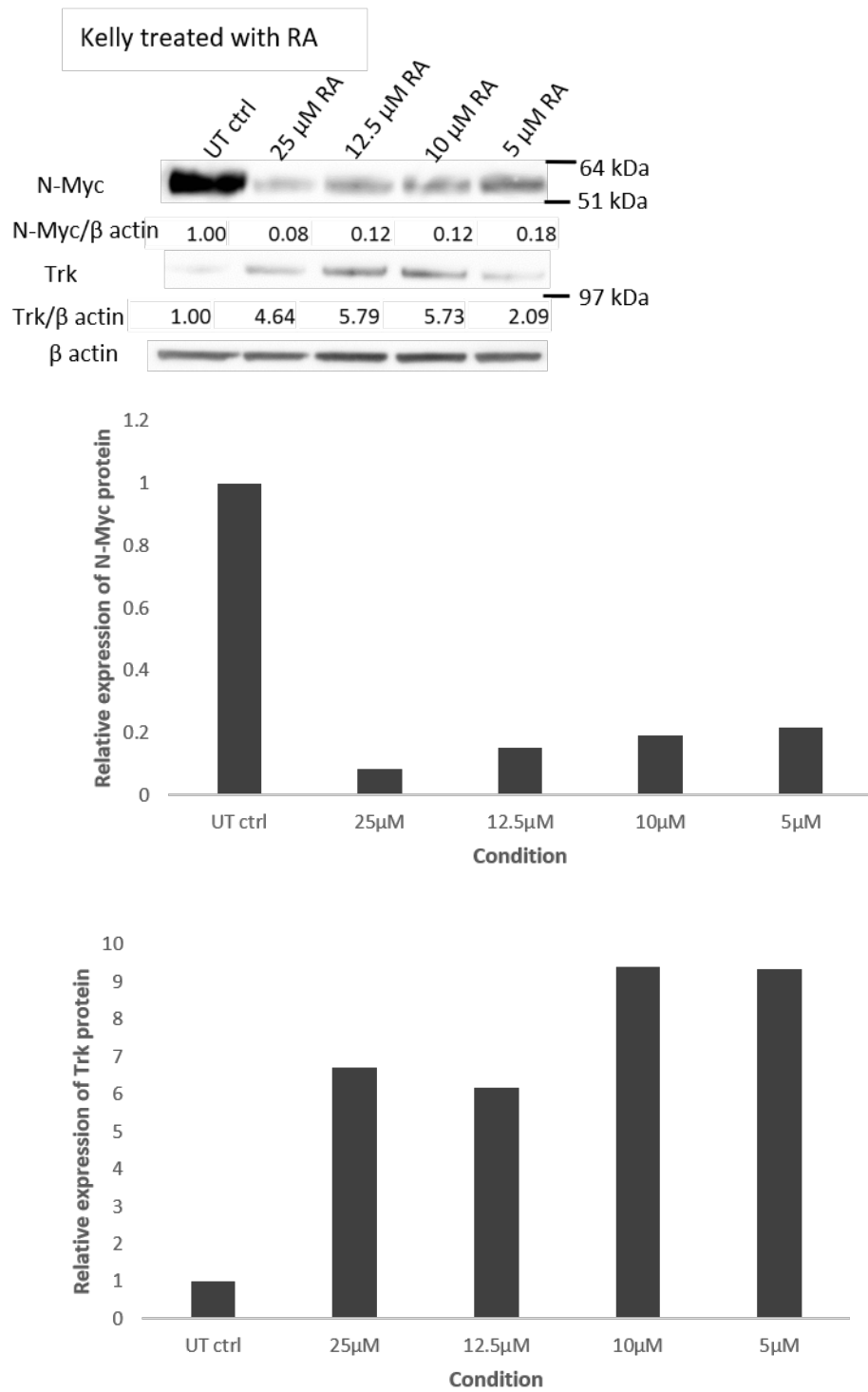
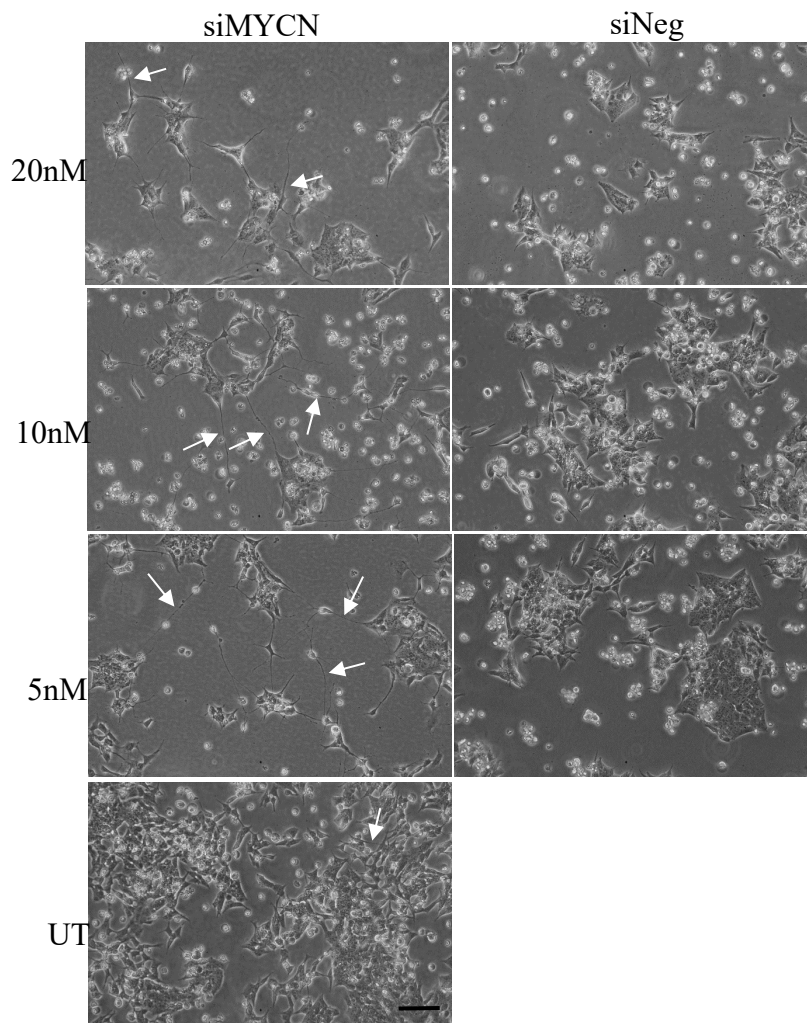


Fig. 4 a)



b)

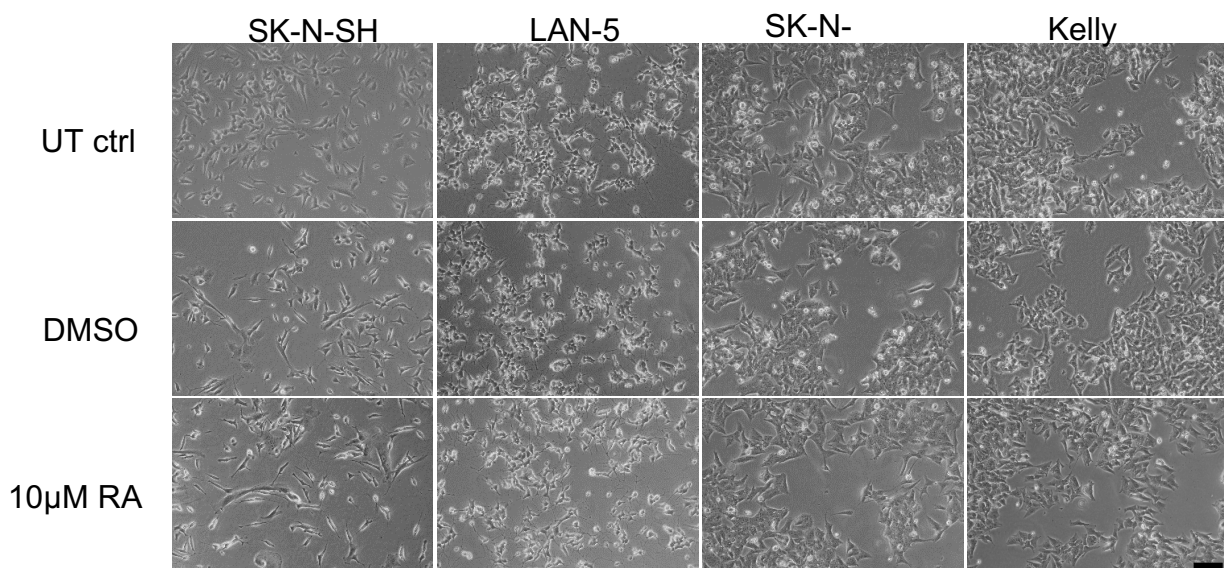
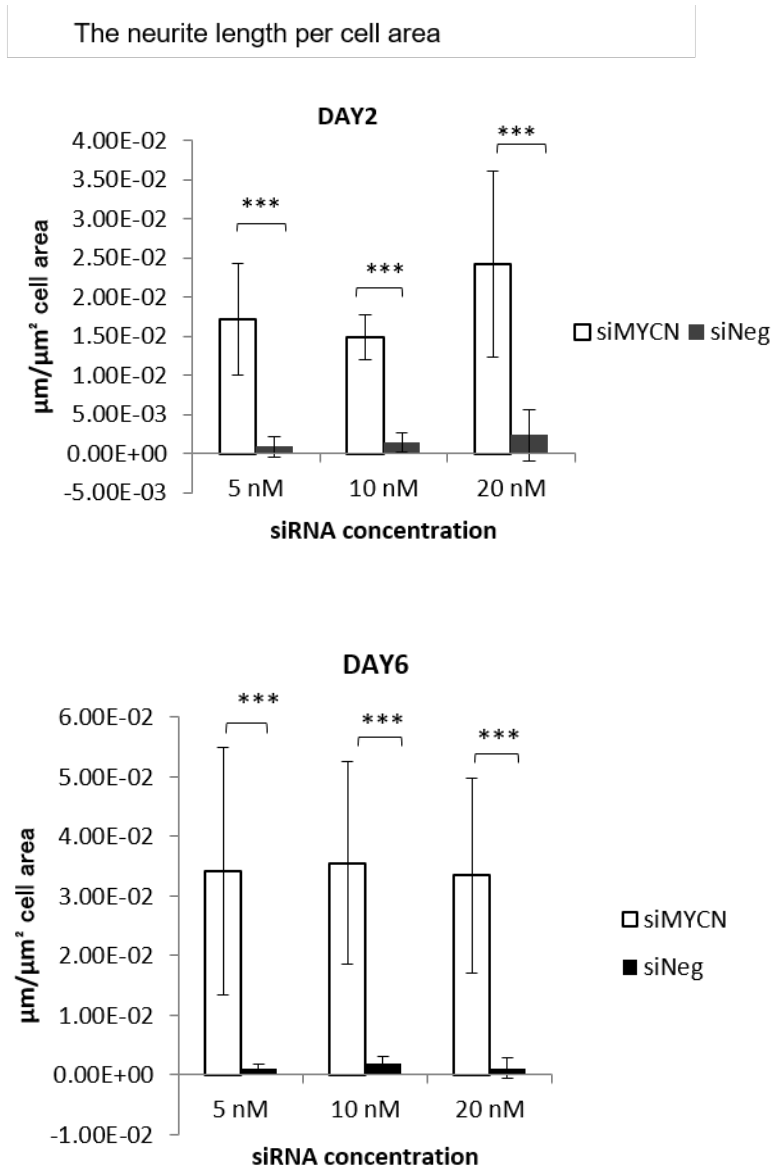


Fig. 5 a)



b)

The number of the neurites per cell area

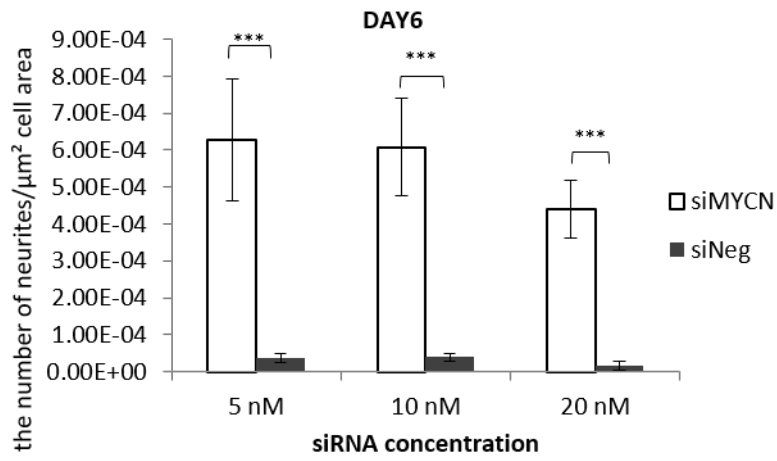
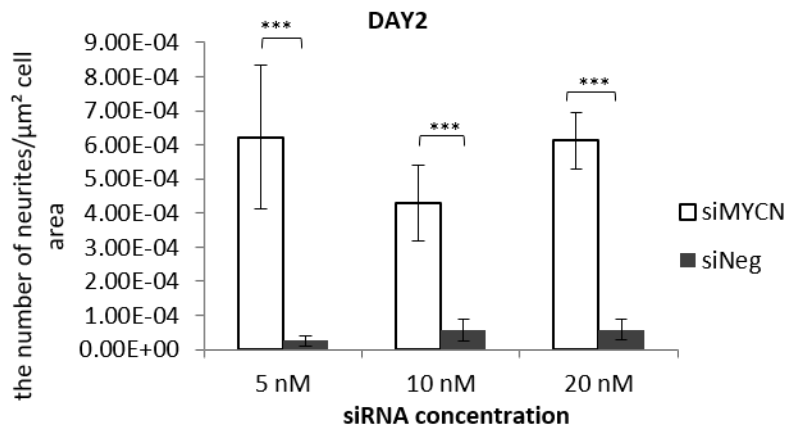
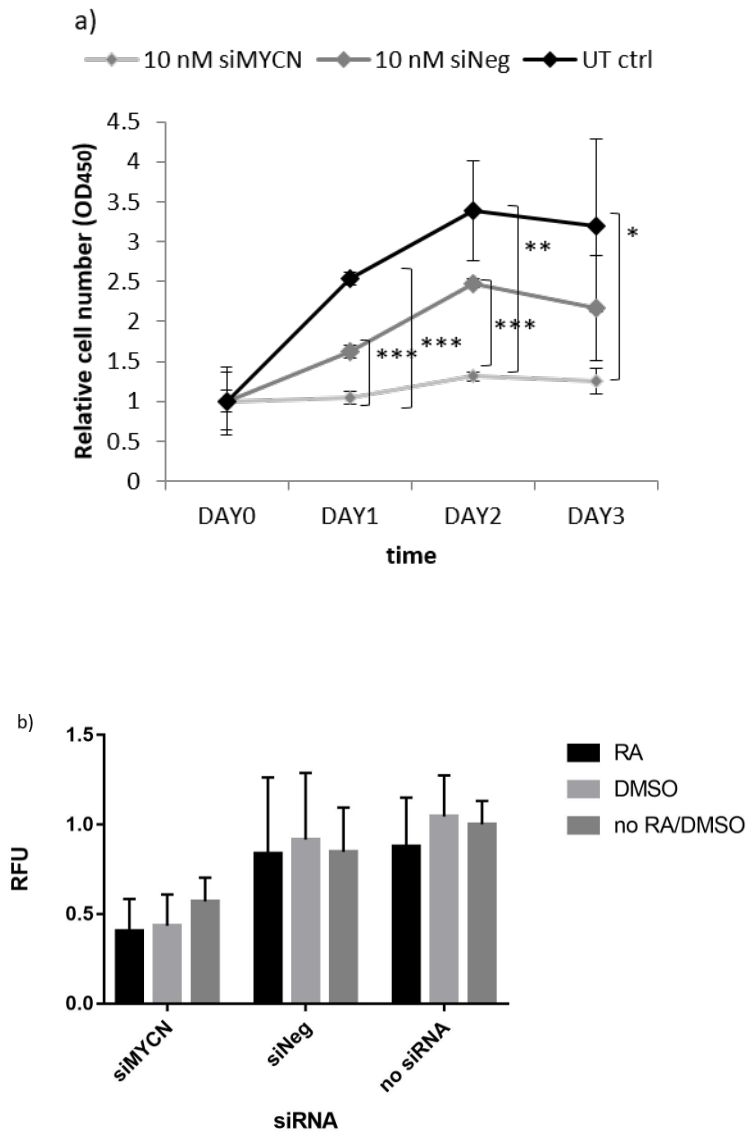


Fig. 6



Pair	significance
siMYCN vs. siNeg+DMSO	**
siMYCN vs. DMSO	***
siMYCN vs. UT ctrl	**
siNeg vs. siMYCN+RA	***
siNeg vs. siMYCN+DMSO	**
RA vs. siMYCN+RA	***
RA vs. siMYCN+DMSO	**
siMYCN+RA vs. siNeg+RA	***
siMYCN+RA vs. siNeg+DMSO	***
siMYCN+RA vs. DMSO	***
siMYCN+RA vs. UT ctrl	***
siNeg+RA vs. siMYCN+DMSO	***
siMYCN+DMSO vs. siNeg+DMSO	***
siMYCN+DMSO vs. DMSO	***
siMYCN+DMSO vs. UT ctrl	***

Table 1. Two-way ANOVA Bonferoni's multiple comparisons test was performed. ** $P < 0.01$, *** $P < 0.001$.

DMSO, dimethyl sulphoxide; RA, retinoic acid; siRNA, short interfering RNA.

Supplementary figures

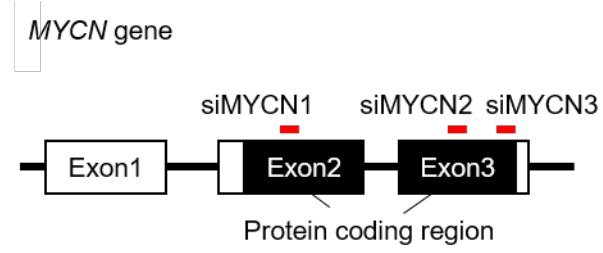


Fig. S1a

Fig. S1b

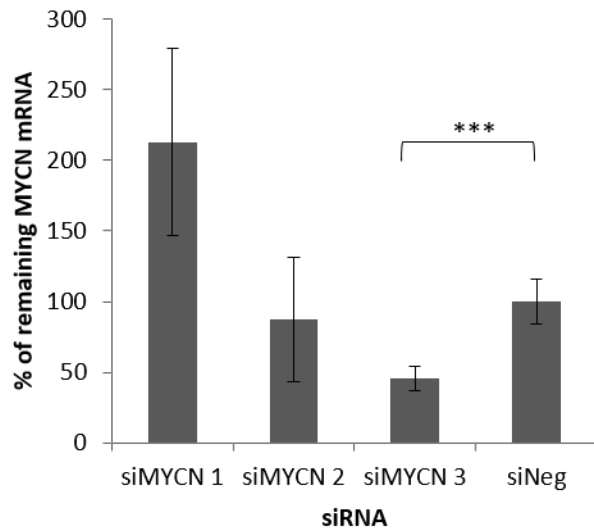


Fig. S2a

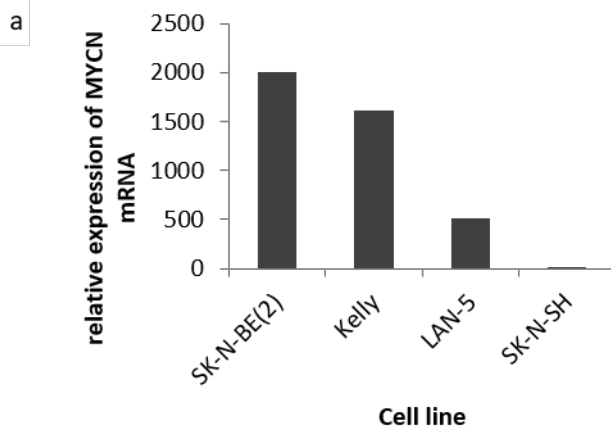


Fig. S2b

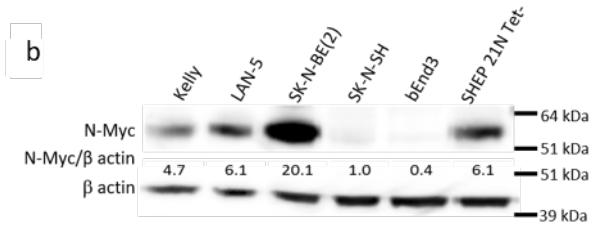


Fig. S3

